

Destructive Physical Analysis of Hollow Cathodes from the Deep Space 1 Flight Spare Ion Engine 30,000 Hr Life Test

IEPC-2005-026

Presented at the 29th International Electric Propulsion Conference, Princeton University,
October 31 – November 4, 2005

Anita Sengupta*

Jet Propulsion Laboratory, Pasadena, CA, 91109, US

Abstract: Destructive physical analysis of the discharge and neutralizer hollow cathode assemblies from the Deep Space 1 Flight Spare 30,000 Hr life test was performed to characterize physical and chemical evidence of operationally induced effects after 30,372 hours of operation with beam extraction. Post-test inspection of the discharge-cathode assembly was subdivided into detailed analyses at the subcomponent level. Detailed materials analysis and optical inspection of the insert, orifice plate, cathode tube, heater, keeper assembly, insulator, and low-voltage propellant isolator were performed. Energy-dispersive X-ray (EDX) and scanning electron microscopy (SEM) analyses were used to determine the extent and composition of regions of net deposition and erosion of both the discharge and neutralizer inserts. A comparative approach with an un-operated 4:1:1 insert was used to determine the extent of impregnate material depletion as a function of depth from the ID surface and axial position from the orifice plate. Analysis results are compared and contrasted with those obtained from similar analyses on components from shorter term tests, and provide insight regarding the prospect for successful longer-term operation consistent with SOA ion engine program life objectives at NASA.

d	=	barium depletion depth
T, T_{insert}	=	insert temperature
A	=	coefficient relating depletion rate to insert temperature
J_{sat}	=	saturation current
e	=	electron charge
k	=	Boltzmann's constant
dt	=	time step
ID	=	inner diameter
SEM	=	scanning electron microscope
EDX	=	energy-dispersive Xray
TH	=	throttle level

I. Introduction

The Extended Life Test (ELT) of the Deep Space 1 (DS1) flight spare ion thruster is the longest operation of an ion thruster processing over 235 kg of Xe propellant and accumulating 30,352 hours of operation during it

* Senior Engineer, Advanced Propulsion Technology, Anita.Sengupta@jpl.nasa.gov

five year run¹. As ion engine life is limited by component level wear and failure mechanisms, the ELT also served as a component level wear test-bed. Specifically, the ELT demonstrated the longest operation to date of a hollow cathode emitter source in a plasma environment with in excess of 30,000 hours on both the discharge and neutralizer cathode assemblies. The test was operated at multiple throttle conditions, however the majority of the time was spent at the full power point, to maximize propellant throughput^{1,2}. As test was concluded prior to thruster failure, 30,472 hours represents the maximum demonstrated life but not the end of life for the NSTAR type discharge cathode. In fact, the discharge cathode showed no change in start behavior or operational performance for the duration of the test suggesting it was not approaching end-of-life. The post test inspection, confirmed this fact revealing an insert surface free from tungstate or oxide layer formation. Similarly the lower current operating neutralizer cathode showed no signs of emitter performance degradation during the test.

A summary of the in-test performance of the discharge and neutralizer cathode is described in sections II and III. The detailed results of the post-test destructive analyses are contained in sections IV and V.

II. Discharge Cathode Operation and Performance

The discharge cathode is the electron source for the NSTAR engine, enabling electron-neutral collisional ionization of the neutral propellant in the discharge chamber. The discharge-cathode assembly consists of the insert (emitter), cathode tube and orifice plate, heater and radiation shield, keeper tube and plate, cathode insulator, low-voltage propellant isolator, propellant-line screen, and associated wiring and stainless-steel propellant line. Figure 1. is an image of the discharge-cathode assembly. A coiled sheath heater is wrapped around the cathode tube and is used to heat the insert during cathode ignition. After the cathode has been ignited, the heater is turned off. The cathode insulator provides isolation between cathode-common-to-keeper and cathode-common-to-anode. The low-voltage propellant isolator, just upstream of the cathode tube, provides isolation between the anode potential feedline and cathode potential. The propellant-line screen, located between the low-voltage propellant isolator and cathode tube, serves as a debris filter and, as will be discussed later, possibly an oxygen (O) getter. The insert consists of a porous tungsten matrix impregnated with a Ba-Ca-Al₂O₃ compound in a 4:1:1 ratio. This compound has a low work function, providing thermionic electron emission from the surface. When heated, barium diffuses to the surface of the insert forming a Barium monolayer from which a reduction reaction takes place. The electrons released in this reaction diffuse to the surface and ionize neutral Xe propellant flowed through the cathode tube².

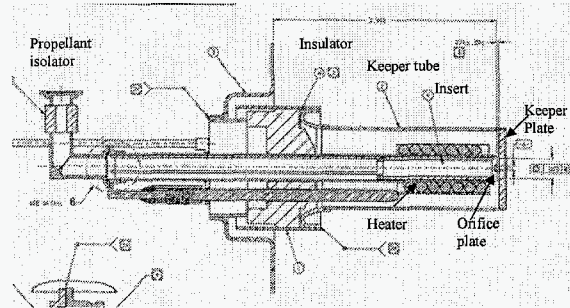


Figure 1. Schematic of the discharge cathode assembly.

A. Wear Mechanisms

Several wear mechanisms exist relating to the discharge-cathode-assembly performance degradation and eventual failure. A leading cause for several of the known failure modes is erosion and eventual removal of the discharge-cathode-keeper plate. Keeper erosion is a well documented wear process for the NSTAR thruster and was tracked photographically during the course of the ELT^{1,3}. Ion-bombardment-sputter-erosion of the keeper plate by the discharge plasma led to the complete removal of the plate after 30,000 hrs of operation. The primary function of the keeper plate is to protect the cathode from discharge-plasma ion-bombardment. As the keeper erodes, it exposes the cathode-orifice plate, heater, and radiation shield to discharge-plasma ion-bombardment. Excessive erosion of the heater may lead to breach of the heater sheath, and therefore heater failure. Heater failure causes cathode failure because without a functioning heater, the cathode cannot be ignited. Keeper erosion can result in orifice-plate removal. During the ELT, following the removal of the keeper, the cathode-orifice-plate-to-tube weld was eroded by discharge-plasma ion-bombardment. If the orifice plate had fallen off, the cathode operation would have ceased. Cathode inability to start due to a cathode-common-keeper short is also a result of wear of the cathode assembly. The source of the shorting material is likely erosion of the discharge-keeper plate^{4,5}. Although not a failure for the cathode itself, erosion of the radiation shield due to discharge-plasma ion-sputtering led to the

formation of tantalum (Ta) flakes large enough that they could lodge themselves between the grids or defocus individual beamlets, causing rogue hole formation.

The other primary cathode wear mechanism, not related to keeper erosion is excessive, is performance degradation or cathode failure-to-start due to insert depletion. Removal of impregnate material is a temperature- and runtime-dependent process. When impregnate material is removed or is not readily available for diffusion to the surface, electron emission cannot occur and the cathode cannot operate.

B. In Test Performance

The ELT discharge cathode operated for a total of 30,472 hrs and was ignited (cycled) 277 times, establishing the ELT as the longest endurance test of a hollow cathode to date. The most significant wear mechanism experienced by the cathode assembly during operation was sputter-erosion of the keeper-electrode plate. Discharge-cathode-keeper erosion is a wear mechanism for ion thrusters, as demonstrated by the previous 8,200 hr test (LDT) of an engineering model thruster (EMT2) and the ELT of FT2^{1,4,5,6}.

After 15,000 hrs of operation, the keeper on FT2 eroded sufficiently to fully expose the cathode heater and cathode-orifice plate to discharge plasma for the remaining 15,000 hrs of the test. Discharge-cathode-keeper erosion was first observed during the TH8 test segment, following a short between cathode keeper and cathode common at 5850 hrs. At that point the keeper began to erode at an observable rate. The intermittent short caused the cathode-keeper voltage to drop from 3.5 V to ~0.4 V. At 8,873 hrs the cathode-keeper-cathode-common short cleared, apparently when the cathode-keeper orifice eroded sufficiently. Cathode-keeper erosion still continued, however, at the subsequent full-power segments, and at a lower rate during TH5 operation. Keeper erosion did essentially stop during TH0 operation from 15,000 to 21,000 hrs^{3,7}.

Figure 2 is a plot of normalized cathode-keeper-orifice diameter versus runtime, and clearly indicates the onset and subsequent power-level-dependence of keeper erosion. It is important to note that this severe keeper erosion was not observed during the first full-power test segment, from 500 to 4500 hrs, or during the previous 8,000-hr endurance test of the EMT^{4,5}, which was operated exclusively at TH15. This suggests that the TH8 operating conditions, the shorted condition, or both initiated the cathode-keeper erosion observed during FT2 testing.

Figure 3 is a photographic comparison of the BOL condition and the EOT condition of the cathode-keeper assembly. All images except the one at 30,352 hrs were taken with the internal tank video system, focused through the optics assembly. Keeper-surface pitting was initially apparent after 5000 hrs of operation. By 10,000 hrs, the keeper plate had eroded significantly, partially exposing the cathode-orifice plate. By 15,000 hrs the keeper-orifice plate had eroded to fully expose the cathode-orifice plate and heater. The image labeled 30,352 hrs was taken after the thruster was removed from the chamber, with the grids removed. This most recent image indicates that the cathode heater and orifice plate had eroded as a result of their exposure to the discharge-chamber plasma for the last 15,000 hrs of operation. This observation will be discussed in more detail in the following sections.

The cause and throttle-level dependence of cathode-keeper erosion are not yet well understood. It may have been the shorted condition that initiated keeper erosion. Results of experimental work discussed in [8,9] indicate that when the keeper is shorted to cathode common, the rate of keeper-orifice-plate erosion is increased over that experienced during a non-shortcd condition.

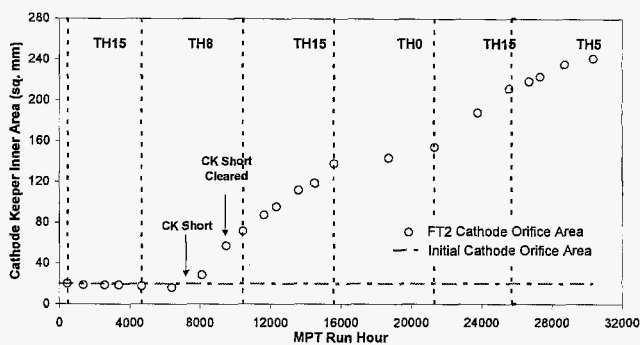


Figure 2. Cathode keeper plate erosion versus runtime.

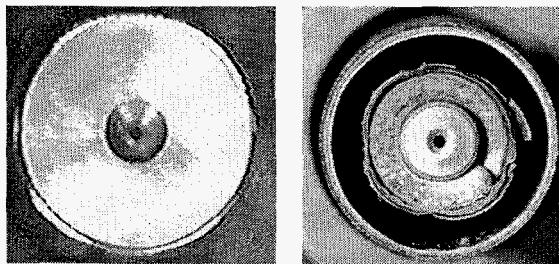


Figure 3. Cathode keeper BOL (left) and after 30,352 Hours of operation (right).

The discharge-cathode-heater power and hot resistance did change with runtime. The heater power began to decrease following a short between cathode common and cathode keeper resulting in a net decrease of 12% from the BOL value by the conclusion of the test. A possible explanation for the heater-power reduction is radiant heat lost to the environment as the keeper orifice enlarged. After 25,000 hrs it is likely the keeper plate had eroded away entirely, resulting in no further change in open area from 25,000 to 30,000 hrs. As a result, steady-state heater power was achieved.

In spite of the severe keeper erosion and degradation in heater performance, the cathode did not experience any noticeable change in its ignition characteristics over its 30,472-hr life. A 250V start voltage was nominally used to ignite the cathode through to the end of the test and ignition time did not vary significantly after a total of 277 restarts of the discharge cathode. This suggests that sensitive cathode-heater components, the cathode orifice, and the cathode insert were not compromised, in spite of the severe keeper erosion and subsequent exposure of the cathode to the discharge-chamber plasma for in excess of 15,000 hrs. The FT2 engine test has therefore set a new minimum lifetime for the hollow-cathode technology of 30,472 hrs total discharge time.

III. Neutralizer Cathode Operation and Performance

The neutralizer cathode is the source of beam-neutralizing electron current to prevent spacecraft charging (Figure 4). Similar to the discharge cathode, the neutralizer is a hollow cathode, with neutral Xe gas flowed through it, inside a cylindrical keeper electrode (anode). The keeper serves two functions: to ignite the cathode during engine start, and to prevent the neutralizer cathode from extinguishing during recycle events, when the high-voltage power supplies are cycled off and on. The keeper power supply maintains the neutralizer current at the fixed level specified in the NSTAR throttle table⁷. The neutralizer-keeper voltage is dependent on the flow rate of Xe through the cathode, the beam current, the keeper current, and the condition of the cathode orifice. Nominal operation of the neutralizer is called spot mode, where the voltage oscillations of the keeper are significantly less than 5 V from peak to peak. Plume mode occurs when the cathode sheath extends to the anode, resulting in large voltage oscillations, an increase in DC voltage, and the production of energetic ions that may have sufficient energy to erode neutralizer surfaces, reducing the lifetime and performance of the neutralizer cathode. Operating with sufficient flow-rate margin and keeper current can prevent plume-mode operation, and to this end the performance of the neutralizer was monitored during the course of the test.

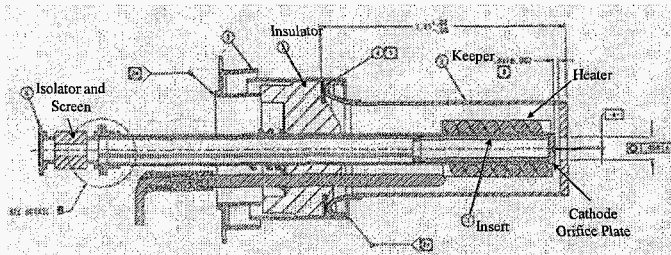


Figure 4. Neutralizer cathode assembly schematic.

Like the discharge cathode, the neutralizer hollow cathode contains a 4:1:1 Ba-Ca-Al-impregnated, porous W insert. The insert is housed inside a MoRe cathode tube with a W orifice plate welded to the downstream end. A swaged heater is wrapped around the cathode tube and is used to heat the impregnate, enabling thermionic emission. Neutral Xe gas is supplied to the cathode fitted with a low-voltage propellant isolator and screen. The cathode tube is enclosed in a concentric cylindrical keeper with a Mo orifice plate ebeam welded to a Ta keeper tube. For FT2 testing, the keeper power supply maintained the neutralizer current at the fixed level specified in the NSTAR throttle table.

Like the discharge cathode, the neutralizer hollow cathode contains a 4:1:1 Ba-Ca-Al-impregnated, porous W insert. The insert is housed inside a MoRe cathode tube with a W orifice plate welded to the downstream end. A swaged heater is wrapped around the cathode tube and is used to heat the impregnate, enabling thermionic emission. Neutral Xe gas is supplied to the cathode fitted with a low-voltage propellant isolator and screen. The cathode tube is enclosed in a concentric cylindrical keeper with a Mo orifice plate ebeam welded to a Ta keeper tube. For FT2 testing, the keeper power supply maintained the neutralizer current at the fixed level specified in the NSTAR throttle table.

C. Wear Mechanisms

Wear mechanisms that limit cathode life specific to the neutralizer assembly include cathode-orifice clogging, cathode-orifice erosion, keeper-tube erosion due to direct-beam ion-impingement, and energetic ion production due to plume-mode operation. Because the neutralizer is a hollow cathode, life limitations include cathode failure-to-start due to impregnate depletion of the emitter, heater failure, and keeper-to-neutralizer-common shorting, as discussed previously.

D. In Test Performance

The AC and DC performance of the neutralizer was monitored throughout the ELT. Neutralizer-keeper voltage and current AC characteristics were monitored on an oscilloscope every 1000 to 2000 hours, to prevent inadvertent operation in plume mode. The neutralizer-keeper DC voltage and current were recorded by the computer data acquisition system every 5 seconds of operation. The neutralizer plume was also monitored using an RPA mounted above the neutralizer in the vacuum test facility, providing a measurement of the neutralizer ion energy distribution. RPA measurements were performed twice during the ELT and are summarized in reference [10]. Every 1000 to 2000 hours of operation, the in situ camera system was also used to inspect the condition of the neutralizer keeper, cathode orifice, and housing.

Figure 5 is a plot of the neutralizer-keeper DC voltage and current versus runtime. The spikes in voltage observed repeatedly over the course of the test correspond to cathode-conditioning events. Cathode conditioning is a process whereby cathode-heater current is applied at various levels to burn off surface contaminants that may have deposited/adsorbed on the cathode surfaces due to exposure to a higher than nominal tank pressure. Higher tank pressure was defined as facility pressure in excess of 1.33×10^{-3} Pa (1×10^{-5} Torr) during a cryopump regeneration or pressure spike. The spikes in the keeper voltage following each conditioning were due to changes to the insert chemistry as a result of the applied heater current.

As mentioned in Section 2, the exposure to a higher background pressure of Xe is not the cause of this discontinuity. Following a cathode conditioning, the keeper voltage tended to return to the preconditioning level until the next cathode conditioning. The voltage spiking was, therefore, a transient effect.

Figure 5 also indicates that neutralizer-keeper performance characteristics were relatively stable during the first three test segments. The neutralizer performance first began to show signs of degradation during the fourth test segment, corresponding to operation at TH0 (0.5 kW). The DC and AC characteristics began to increase 800 hrs into TH0 operation, and deposits began to form within the orifice, as documented by the in situ camera system. By the conclusion of the 5700-hr TH0 segment, internal tank video inspections revealed that the orifice was over 50% blocked (Figure 5.2-3), and the flow-rate margin from plume mode had dropped to below acceptable levels at the nominal flow-rate setpoint. It is theorized that the deposits in the orifice are responsible for the degradation in neutralizer performance, further supported by the results of the subsequent TH15 operation. The thruster was returned to full-power operation following the TH0 test segment, and remained at the TH15 power point for approximately 5000 hrs. During this test segment, the deposits within the orifice were removed, and the TH0 keeper-voltage characteristics and flow-rate margin from plume mode returned to nominal levels. This suggests that operation at the higher power level removed the deposits, and that the deposition mechanism is likely power-level-dependent, specifically manifesting itself during low-power operation. This suggests a temperature-dependence to the orifice-clogging mechanism, with hotter operation eliminating orifice deposits.

A similar phenomenon was observed during the DS1 mission, when the flight neutralizer exhibited signs of plume-mode operation following extended operation at 0.54 kW (ML1 ~ TH1). Extensive ground and in-flight tests with the respective engines were performed at that time to characterize the flow-rate and keeper-current dependence on plume-mode operation. Analysis of data from the RPA diagnostic available both on the DS1 spacecraft and in the ELT test facility indicated that increasing keeper current and/or increasing flow rate through the neutralizer reduces energetic ion production and increases margin from plume-mode operation. Based on these results, the neutralizer flow rate was increased for DS1 for all lower power throttle levels. Similarly, the neutralizer-keeper current was increased for the final ELT test segment at TH5 (1.1 kW) from 2.0 A to 2.4 A to provide additional margin from plume-mode operation and to counteract the orifice-clogging mechanism, which is likely temperature-dependent. Increasing the keeper current will allow the keeper to run hotter. The TH5 power level was specifically chosen to investigate the power-level dependence of neutralizer performance degradation. Details of these tests can be found in reference [10].

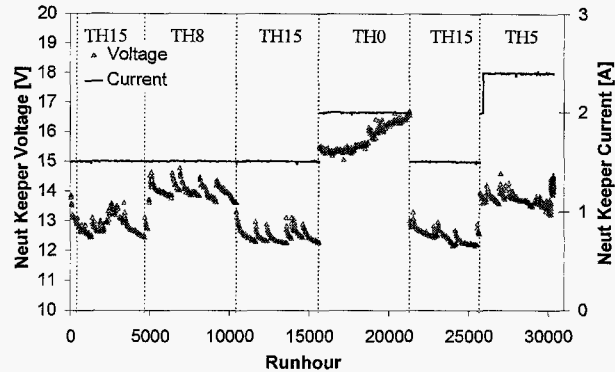


Figure 5. Neutralizer keeper voltage and current versus runtime.

IV. Discharge Cathode Post Test Inspection

Post-test inspection of the discharge-cathode assembly was subdivided into detailed analyses at the subcomponent level. Detailed materials analysis and optical inspection of the insert, orifice plate, cathode tube, heater, keeper assembly, insulator, and low-voltage propellant isolator were performed. Energy-dispersive X-ray (EDX) and scanning electron microscopy (SEM) analyses were used to determine the extent and composition of regions of net deposition and erosion. Laser profilometer scans of the cathode-orifice-plate surface were obtained to quantify mass loss and eroded depth. Critical findings are discussed in the sections immediately following.

A. Insert Analysis

A detailed analysis of the fracture surface of the discharge-cathode insert was performed. The primary objectives of the analysis were to quantify impregnate depletion as a function of position and depth from the inner diameter (ID) surface, to quantify tungstate formation or the presence of other poisoning layers, and to document tungsten transport within the cathode assembly.

The post-test condition of the insert was documented after removal from the cathode tube. The post-test condition of the exterior and interior can be seen in Figure 6. The white crust on the exterior surface is barium oxide (BaO) migrated from the tungsten matrix. The BaO layer was present at all but the upstream end of the insert, where the temperature is expected to be lowest. The post-test condition of the insert interior can be seen in greater detail in Figure 7. Heavy crystal deposition was apparent at the downstream end, with significantly less in the upstream direction. This observation will be discussed in more detail in the following sections.

The fractured insert geometry allows analysis of chemical composition at the ID surface and as a function of depth from the ID surface. SEM and EDX analyses were used to probe the fracture surface of both the 30,000-hr ELT insert and an unused 4:1:1 insert, to provide a comparative estimate of impregnate depletion and surface-chemistry changes. SEM inspection of the insert revealed heavy tungsten crystallite deposition at the extreme downstream end, nearest the orifice plate. Figure 8 shows the tungsten crystals and a relative coverage area of 30–40% of the tungsten matrix below, at the downstream end. It should also be noted that apart from the tungsten crystallites, tungstates and other oxide/poisoning layers were not detected on the entirety of the surface. This is a critical finding, for oxide layers and tungstate formation are typically responsible for limiting cathode life by preventing BaO migration to the surface and consequently reducing the reaction that allows for thermionic emission. SEM inspection of the insert surface midway along its length revealed no tungsten crystallite formation and no oxide layers (Figure 9). SEM inspection at the upstream end of the ID surface revealed molybdenum oxide (MoO) deposits in the vicinity of the Mo collar (Figure 10). Crystallite formation was also not present at the upstream end.

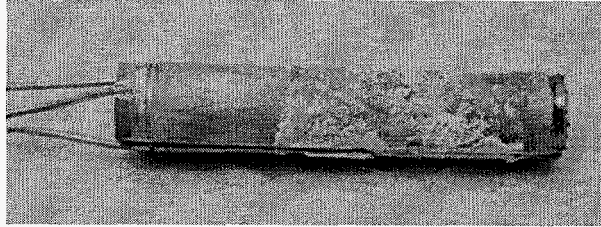


Figure 6. The exterior surface of the discharge cathode insert after 30,352 hours of operation.

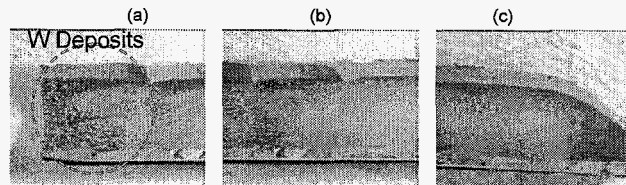


Figure 7. Insert ID surface from (a) downstream, (b) middle, and (c) upstream.

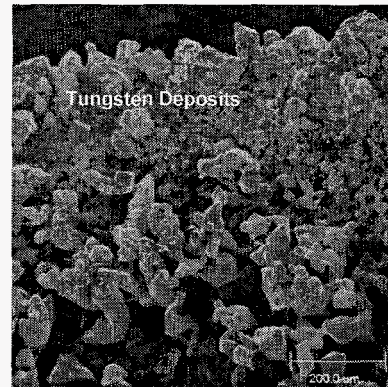


Figure 8. Insert ID at the downstream end showing tungsten crystallites.

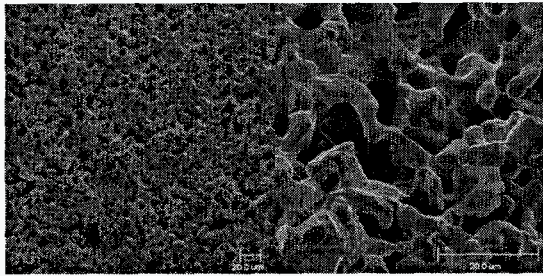


Figure 9. Insert ID surface at middle showing absence of crystallite formation at different magnifications.

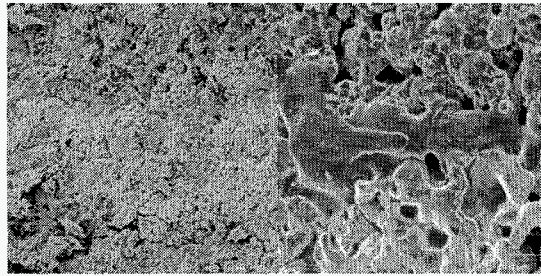


Figure 10. Insert ID surface at downstream end showing MoO deposits at different magnifications.

Figure 11 shows the ID surface of the unused insert to the ID surface of the ELT insert at several axial locations. The white substance present in the tungsten matrix of the unoperated ID surface is the impregnate material. The impregnate is not present at the ID of the ELT insert: it has been depleted due to operation. As will be discussed in the next section, although depleted at the surface, the impregnate material is present in the subsurface of the matrix of the ELT insert, available for evaporation to the surface during cathode operation.

EDX analysis was used to measure impregnate depletion. This was accomplished by measuring the relative signal strengths for Barium and tungsten at several different locations for each insert. Ba:W ratio measurements for the control insert at different depths from the ID surface were used as the baseline for the absence of impregnate depletion at a given depth and were compared to the ELT insert. Figure 12 compares the Ba:W ratio versus depth from the ID surface. Using the metric described above, the impregnate material depletion depth was calculated as a function of axial distance from the orifice plate (downstream end) and is shown in Figure 13.

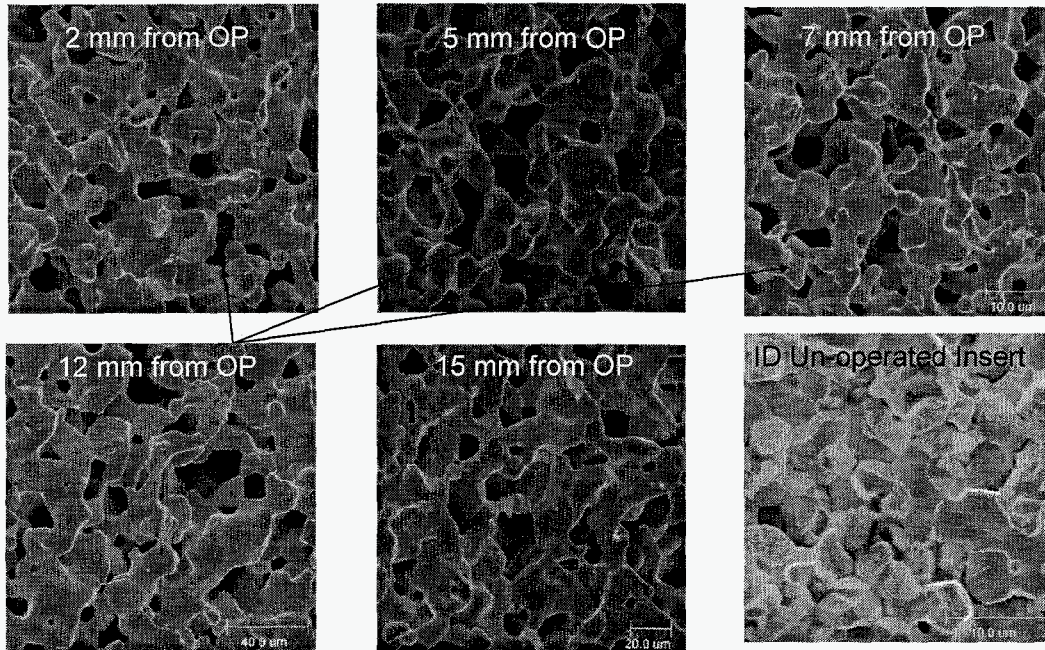


Figure 11. Axial variation of ID surface for ELT insert given as distance from orifice plate (OP) compared to the nominal ID surface of the control insert.

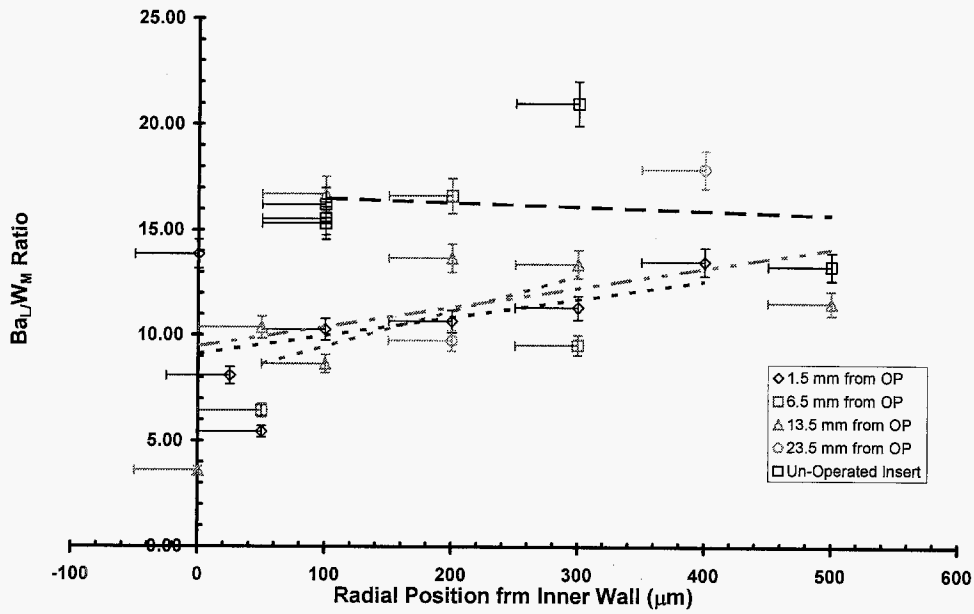


Figure 12. Ba:W ratio variation from the ID surface for the ELT and control insert

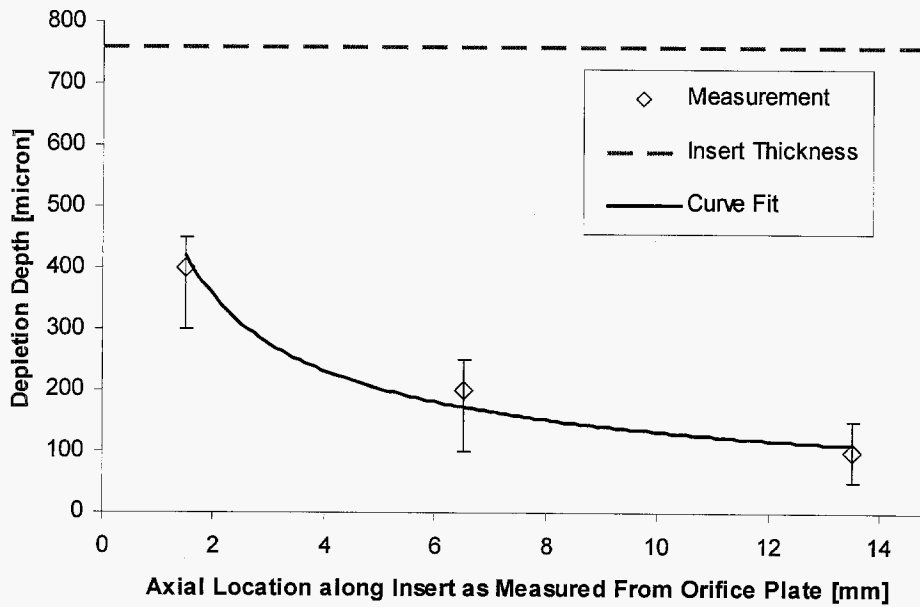


Figure 13. Ba:W ratio variation from the ID surface for the ELT and control insert

The insert was more heavily depleted at the downstream end, exhibiting a nonlinear decrease with axial distance from the orifice plate. At the downstream end, the insert was depleted to $400 (\pm 50) \mu\text{m}$, which is equivalent to 52% of the total insert thickness. At 13.5 mm upstream from the orifice plate, the insert was depleted by only 13%. Figure 14 is a comparison of the subsurface insert fracture surface for the ELT and control insert. Impregnate material (white substance) can be seen in the subsurface material, corresponding to the Ba:W measurements. Although partially depleted, the ELT cathode insert operated nominally through to the conclusion of the test,

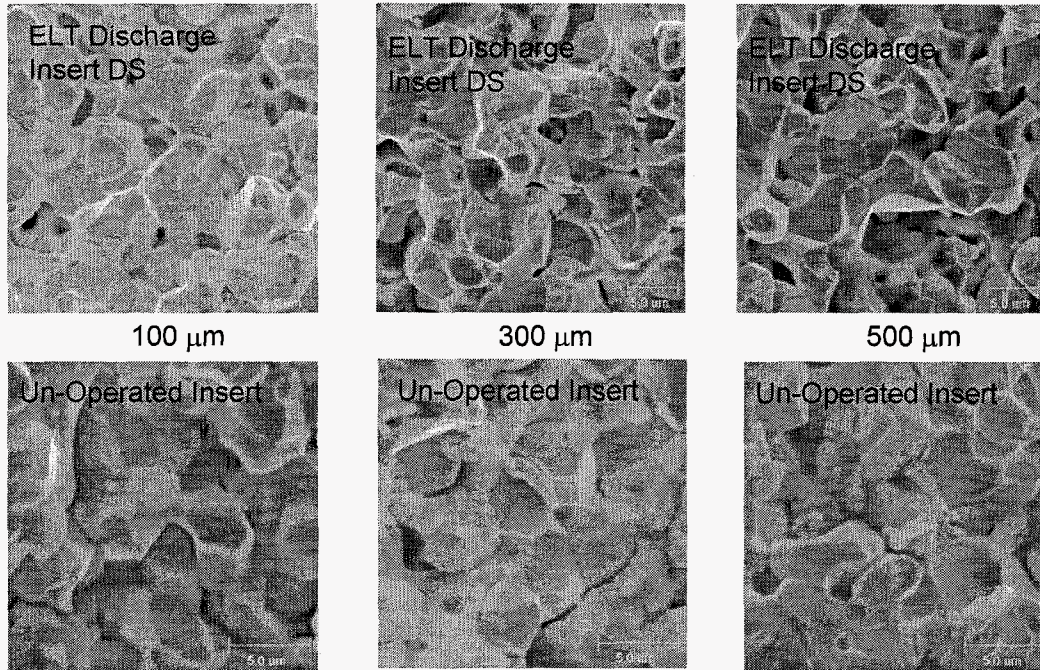


Figure 14. Comparison of ELT and control insert downstream fracture surface as a function of depth from the ID surface

suggesting that the subsurface impregnate material was available for diffusion to the surface, enabling thermionic emission. Palluel and Shroff investigated cathode life as a function of barium evaporation rate. They established an empirical relationship between Barium depletion depth, insert operating temperature, and cathode runtime¹¹:

$$d = A(T)t^{\frac{1}{2}} \quad (1)$$

In equation (1), depletion depth (d) is proportional to the square root of the runtime (t) and a proportionality constant dependent upon the operation temperature ($A(T)$). The cathode operating temperature can be computed via the Richardson equation¹¹:

$$J_{sat} = 120T_{insert}^2 \exp\left(\frac{e\phi_e}{kT_{insert}}\right) \quad (2)$$

In equation (2), the current density at saturation is a function of the temperature of the insert and the cathode sheath potential. Using the equations above, the empirical constants from [11], and the runtimes and current densities at the ELT throttled operating conditions, it is estimated the ELT cathode had an additional $25 (\pm 5)$ hrs of operation at TH15 prior to complete impregnate depletion. This lifetime estimate assumes that Barium (impregnate) depletion

due to evaporation is the life-limiting mechanism for hollow-cathode operation. Other life-limiting factors not reflected in equation (1) include clogging of the tungsten matrix with crystallites that might prevent the diffusion of BaO to the surface, the chemical unavailability of subsurface BaO due to tungstate formation within the matrix, or the poisoning of the cathode due to impurities in the feed system that can form poisoning layers. These factors are more difficult to quantify than is Barium depletion; however, after 30,000 hrs of operation, there was no evidence that these other life-limiting factors were occurring within the ELT discharge-cathode insert.

In summary, the findings of the ELT discharge-cathode-insert analysis indicate a surface free from oxide/poisoning layers, with tungsten crystallite growth on the surface most apparent at the downstream end, absence of tungstate formation, axially dependent impregnate depletion, significant quantities of impregnate material in the subsurface tungsten matrix, and nominal cathode operation throughout the duration of the test.

B. Cathode Tube

Post-test examination of the discharge-cathode-keeper tube is shown in Figure 15. The image shows the post-test condition of the cathode tube interior. Examination of the discharge-cathode tube revealed a significant quantity of BaO on the ID surface. The origin of the BaO is the insert itself, which had fused to the interior surface of the cathode tube. The trend noted was increasing BaO deposition in the downstream direction, which corresponds to the higher temperature. MoO deposits were found at the upstream end of the tube, likely from the Mo collar that is located concentric to this region. There was no measurable erosion to the cathode tube, only net deposition on the interior.

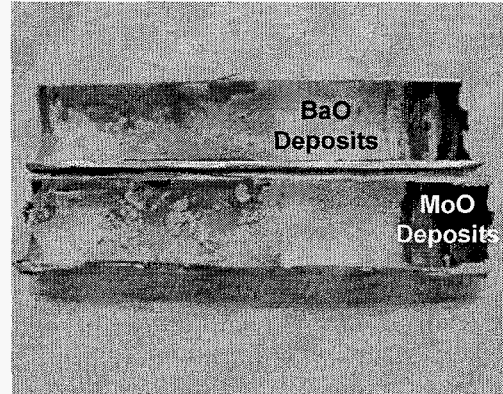


Figure 15. Post test condition of the cathode tube interior showing BaO and MoO deposits.

C. Cathode-Orifice Plate

Post-test examination of the cathode-orifice plate revealed that surface erosion of the orifice plate was more severe than was previously surmised from the in situ photography taken during the test. The cathode-orifice-plate-to-cathode-tube electronic-beam weld joint was fully removed by ion-bombardment sputter-erosion of the plate surface after 30,000 hrs of operation. The weld was initially located on the side of the plate, at the midway point through the thickness dimension. By the conclusion of the test, the periphery of the plate was only 28% of the BOL plate thickness (Figure. 16). Although the weld joint was fully removed by sputter-erosion, the orifice plate was still adhering to the cathode-tube wall and ledge at the conclusion of the test. SEM analysis indicates that this adherence was due to a 20-to-50- μm -wide area of fusion between the molybdenum-rhenium (MoRe) cathode tube and tungsten orifice plate. If not for this small area of thermally induced fusion, the plate may have fallen off, resulting in cathode

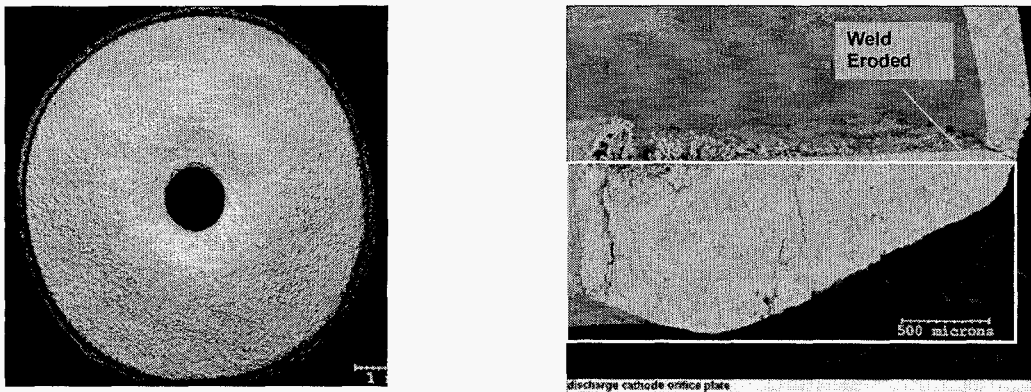


Figure 16. Post test condition of the cathode orifice plate showing the (left) downstream side and (right) cross sectional view of orifice and tube connection. The box indicates the pre-test geometry of the plate.

failure. This is a key finding of the ELT, in that minimizing cathode-keeper erosion to prevent ion-bombardment of the orifice plate is essential to prevent premature cathode failure. Laser profilometer scans across the surface provided revealed that approximately 128 mg of the tungsten plate had eroded after 30,000 hrs of operation.

Examination of the upstream surface of the cathode-orifice plate revealed heavy deposition of tungsten on the plate surface and inside the orifice channel. Figure 17 compares the post-test condition of the upstream ELT orifice with the upstream orifice of an unoperated cathode-orifice-plate. The tungsten crystallite density was highest in the vicinity of the orifice, forming a smooth region that extended from the orifice radially from the center. From 0.37 mm to 0.717 mm radially from the orifice, the deposit consisted of individual, large tungsten crystals. Beyond this, smaller particle deposits of both tungsten and Barium were scattered from 0.717 mm to several mm out radially. Dense tungsten deposition also occurred within the orifice, reaching a maximum thickness of 50 μm on the channel wall. The composition of the orifice deposit is predominantly tungsten, with an increasing Mo content towards the ID of the deposit.

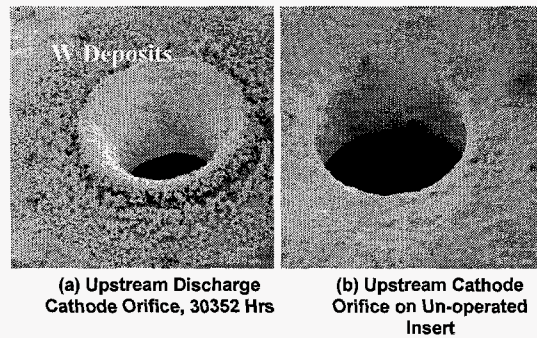


Figure 17. Comparison of upstream (a) ELT and (b) un-operated cathode orifice plate.

D. Cathode Keeper Tube

Post-test examination of the discharge-cathode-keeper assembly confirmed the complete removal of the keeper plate due to sputter-erosion during the test. Examination of the keeper tube revealed significant erosion of the inner-wall thickness at downstream end (Figure 18). The maximum erosion occurred 2.5 mm from the downstream end, where up to 47% of the wall thickness was removed. In addition to the net erosion, deposits of varying morphology were also found adhered to the interior of the cathode tube. The deposits were primarily Ta but had increasing Mo content and striated appearance in the upstream direction. In addition to these deposits, a few large Ta pieces were also found fused to the interior of the downstream tube wall. The source of the large Ta deposits is likely flaking of the discharge-cathode-heater radiation shield, which occurred after there was sufficient erosion of the cathode-keeper plate to expose the radiation shield to the main discharge plasma. The large Ta flakes were a few mm long, large enough to cause a grid-to-grid short and/or severe ion-impingement of the accelerator grid. The flaking of the radiation shield, a direct result of keeper erosion, represents a previously underappreciated mechanism that could potentially lead to an unclearable grid-to-grid short or rogue holes.

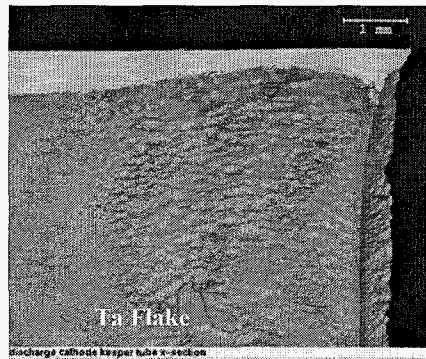


Figure 18. Erosion of the interior downstream end of the keeper tube.

E. Cathode Heater

Post-test examination of the cathode heater revealed significant sputter-erosion and Ta crystallite growth on the surface of the downstream coil. The source of the crystallites is sputter eroded heater-sheath Ta that re-deposited on the heater sheath. Only the last coil exhibited erosion, for it was exposed to discharge-plasma ion-bombardment following removal of the keeper plate. Figure 19 is a cross section of the discharge heater of the eroded downstream (last) coil. The magnesium oxide (MgO) insulating layer and center conductor dimensions and appearance were nominal in the eroded heater cross-section. The outer Ta sheath eroded up to 150 μm from nominal wall thickness as compared to an uneroded cross-section. The sheath also exhibited surface cracking in several locations, but EDX scans confirmed no migration of the MgO insulator through the sheath anywhere in the eroded region .

The post-test condition of the discharge heater was determined by energizing it under vacuum (prior to sectioning) and monitoring its thermal response with an infrared (IR) camera: hot spots or large temperature fluctuations can

indicate that a heater's internal structure has degraded. There was no difference in transient and steady-state performance at 3 A between the two heaters. It should be noted that in a previous test the neutralizer heater exhibited performance identical to that of an unused heater, therefore establishing its operation as nominal. Temperature variations along the heater were less than 50°C, consistent with the control heater thermal variation, confirming that the heater operation and internal structure had not been compromised due to extended use or erosion. Tests were also performed after painting black dots onto each coil of the heater to ensure that a uniform surface emissivity was seen by the IR camera. Experiments with the painted heater yielded data similar to the unpainted heater data and also did not indicate heater degradation.

F. Propellant Line Screen

The propellant-line screen is part of the low-voltage propellant-isolator assembly. Located just upstream of the ceramic isolator, it serves as a debris filter and prevents plasma from getting into the isolator. Post-test examination of the screen revealed arcing tracking, as shown in Figure 20. SEM inspection revealed regions where the stainless-steel wires melted due to some type of localized high-temperature exposure. Chemical analysis of the screen indicated that the upstream side of the screen was coated with iron oxide (FeO). Analysis of the downstream side indicated a surface-deposit composition of primarily BaO as well as some FeO, but less than the upstream side.

G. Low Voltage Propellant Isolator

Post-test examination of the low-voltage propellant-isolator assembly also revealed evidence of arcing, suggesting operation outside of its design envelope (Figure 21). Arc tracking and melting were observed on the discharge propellant-line screen, as mentioned previously. Post-test inspection of the ceramic-to-metal braze joints also revealed evidence of high-temperature exposure, with a submicron-thick deposit of nickel (Ni) and copper (Cu) braze material along the entire length of the ceramic, and large deposits of braze material in the right-angle adapter. This is critical, for during the ELT, the impedance between cathode and anode varied dramatically from the GΩ's at BOL to MΩ's at EOT. It is likely that this layer of redeposited Ni and Cu braze was the conductive path from cathode common to anode, which manifested itself during the test as a varying resistance between these two points. It is believed that an electrical discharge through the isolator is responsible for this arc damage. The low-voltage isolator is designed to reliably stand off about 100 V. In normal operation it must stand off the cathode-to-anode potential of approximately 25 V, well within its capability. However, during an engine restart procedure, 250 V was nominally used to ignite the cathode. At the beginning of the test, a more flight-like start circuit was used that applied a 650-V pulse between cathode and anode. For one or more of these reasons, it is likely that operation beyond the design limit of the isolator resulted in arcing across it during the ELT. X-ray examination of the isolator confirms that the ceramic and propellant-line connections were intact at the conclusion of the test. Therefore the use of the low-voltage propellant isolator in the NSTAR thruster represents a potential failure mechanism due to braze-joint failure.

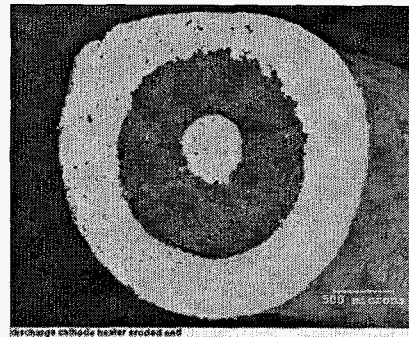


Figure 19. Cross section of eroded heater coil.

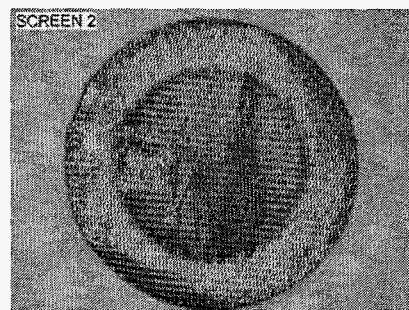


Figure 20. Upstream side of propellant line screen.

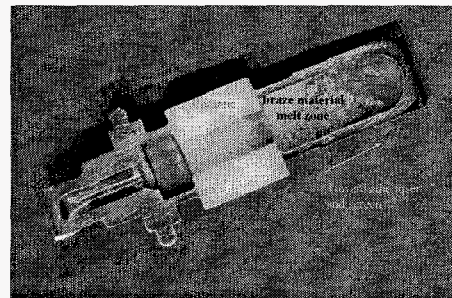


Figure 21. Cross section of the low voltage propellant isolator.

H. Cathode Insulator

Post-test examination of the cathode insulator revealed C deposition on the downstream surface (Figure 22). Although the deposit was measurable (microns thick), it did not provide a conductive path from the cathode-common-potential inner tube to the concentric keeper-potential tube or anode-potential collar. Therefore, the C deposition was not responsible for the cathode-to-anode impedance degradation and variation measured during the course of the test.

V. Neutralizer Cathode Post Test Inspection

Post-test inspection of the neutralizer-cathode assembly yielded several findings with regards to net erosion and deposition of key components. The post-test inspection included detailed physical and materials-analysis of the insert fracture surface, keeper tube and plate, orifice plate and channel, ceramic insulator, and heater. Key findings will be presented in the following sections.

A. Insert Analysis

Analysis of the fracture surface of the neutralizer insert was performed by Georgia Institute of Technology. Unlike the discharge cathode insert, the outer diameter (OD) surface of the neutralizer-cathode insert was clean, with no BaO deposition (Figure 23). The neutralizer insert had significantly less W crystallite deposition than did the discharge cathode insert described previously. Figure 23 is a comparison of the insert fracture surface at 100, 350, and 500 μm from the ID surface. The unoperated insert at 100 μm from the ID surface is shown for comparison. Impregnate material depletion is evident at 100 and 350 μm from the ID surface though this depletion is less than that for the discharge-cathode insert. Figure 25 is a comparison of the Ba:W ratio for the unoperated insert and the neutralizer insert at the downstream end, as a function of depth from the surface. Like the cathode insert, the neutralizer insert surface was depleted of impregnate material relative to the unoperated insert. Impregnate material found roughly 300 μm from the surface of the neutralizer insert was equivalent to that found in the unoperated insert at the same depth, and the neutralizer insert had a greater signal strength than the unoperated insert. This is equivalent to 40% depletion from the ID surface.

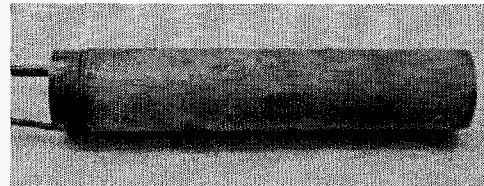


Figure 22. Post test condition of the neutralizer insert.

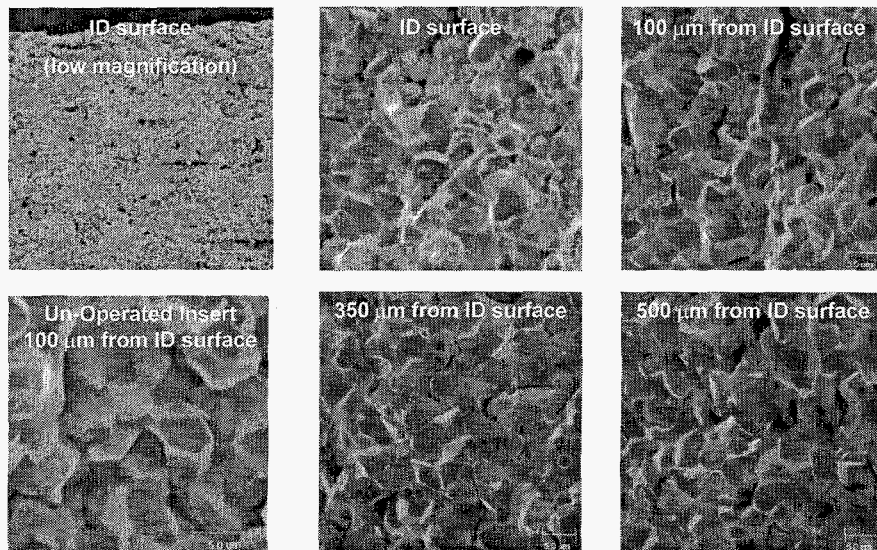


Figure 23. Neutralizer insert fracture surface at different depths from the ID surface.

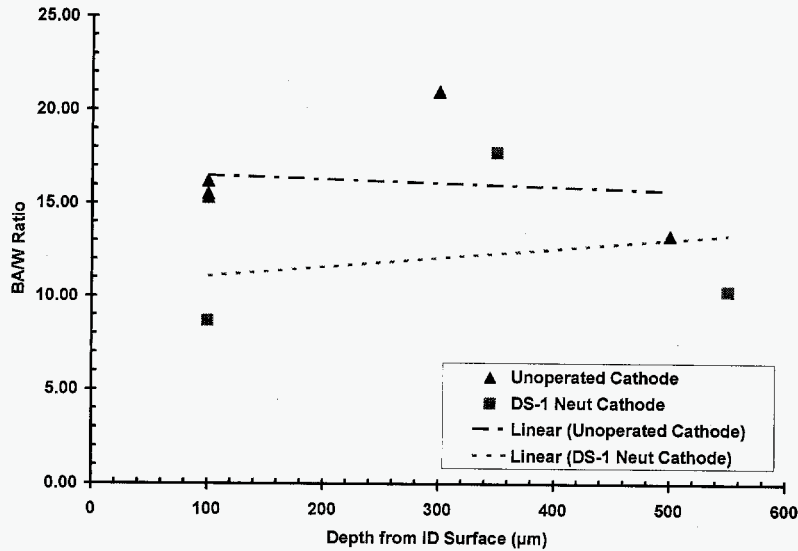


Figure 24. Comparison of Ba:W ratio measurements with depth for the ID surface for the neutralizer and un-operated insert.

Overall, the post-test condition of the neutralizer insert, similar to that of the discharge-cathode insert in the absence of oxide layers and limited impregnate depletion, suggests that the neutralizer insert was healthy and fully functional as an electron emitter throughout the life test. W deposition, however, was significantly less than that observed on the discharge-cathode insert and cathode-orifice plate. The comparatively lower W deposition and impregnate depletion is thought to be consistent with the lower-current operation and therefore lower temperature of the neutralizer insert.

B. Keeper Assembly

Post-test examination of the neutralizer-keeper tube indicated significant erosion of the wall thickness on the beam-exposed side. Measurements indicate that the beam-exposed tube had eroded up to 20% from the nominal wall thickness at the downstream end (Figure 25)^{1,2}. This erosion is the result of direct ion-impingement and is proportional to the beam voltage, providing a potential failure mode for higher-specific-impulse thruster designs. The non-exposed side of the keeper tube and the downstream face of the keeper plate had a primarily carbon coating up to 16 μm thick, the result of re-deposition of facility material in the thruster plane. The interior of the keeper tube was also examined under the SEM. Submicron-thick layers of Mo, Re, and stainless elements were deposited in bands on the ID surface. The composition varied with increasing stainless content and with proximity to the keeper plate. No net erosion of the keeper-tube interior was measured.

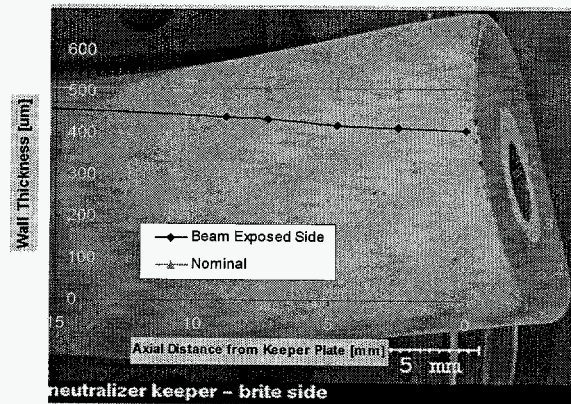


Figure 25. Neutralizer keeper tube post test condition overlaid with erosion profile.

Post-test inspection of the upstream side of the neutralizer-keeper plate indicated a coating on the entire surface. The coating was partially flaking in some locations. The coating was composed of stainless-steel elements, C, and W. A semi-quantitative analysis of the coating indicated that it was 80% C and therefore a facility-induced effect.

SEM inspection of the aperture in the neutralizer-keeper plate also revealed the presence of net deposition. The two-layer deposit was composed of a dense W layer, followed by much thicker but less dense W follicle layer. Comparison of the post-test condition of the ELT keeper aperture with that of the LDT aperture indicates a similar dense W layer in each. However, W follicles were present only in the ELT keeper plate orifice. These follicles may therefore be related to, or be similar in composition to, the deposits observed in the neutralizer-cathode orifice during the TH0 segment of the ELT. Detailed compositional analysis of the deposited layer indicates an increasing stainless content with depth from the ID surface.

C. Cathode-Orifice Plate

SEM inspection of the neutralizer-orifice plate and channel revealed the absence of erosion in the thickness dimension, no erosion of the plate-to-tube weld, and no evidence of the deposits that clogged the orifice, previously photographed during the TH0 test segment (Figure 26). The orifice channel exhibited net erosion, as seen in Figure 5.2 26a. Comparison of the net erosion of the 30,352-hr ELT with that of the 8,000-hr LDT neutralizer orifice indicates that the profile and magnitude are identical⁵. Therefore, neutralizer-orifice erosion essentially stopped at or before 8,000 hrs of operation. The morphology and geometry of the surface indicate that the chamfer section did not experience any net erosion and its roughened appearance is consistent with a chemically etched surface. The channel section, however has a smooth, crystallite-structure surface, a result of net erosion of the thoriated-tungsten matrix.

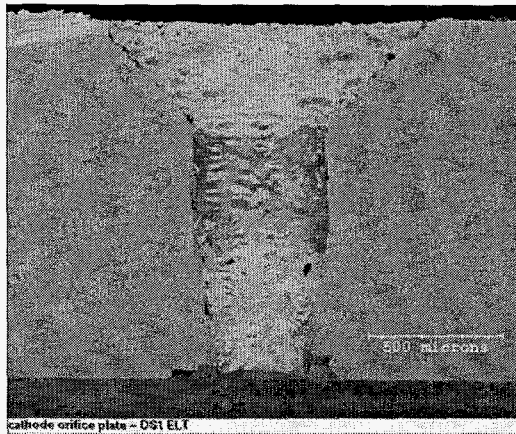


Figure 26. Neutralizer keeper tube post test condition overlaid with erosion profile.

The upstream surface of the cathode-orifice plate was relatively clean. A ring of BaO particles was present where the insert cylinder contacted the plate in the assembled configuration and a few tungsten particles were also found on the surface. Overall the plate was clean, in stark contrast to the discharge-cathode-orifice plate.

D. Cathode Heater

Post-test inspection of the neutralizer-cathode heater and radiation shield indicated no sputter-erosion of either part. Post-test inspection of the cathode tube exterior indicated a brown discoloration on the tube outer diameter surface in the vicinity of the ceramic. This discoloration is barium, the source of which can only be the insert. It is unknown how barium could have deposited here. IR vacuum testing revealed that transient and steady-state performance of the energized neutralizer heater was similar to that of a control heater. Temperature variations on the heater and over the individual coils were less than 50°C.

E. Cathode Insulator

Post-test inspection of the neutralizer insulator was focused on understanding the cause of the impedance degradations experienced during the test. Minimal but measurable sputter-deposition of Ta and MoRe from the cathode and keeper tubes was found on the downstream surface of the ceramic in the vicinity of the cathode tube. These deposits did not extend to the surrounding keeper tube and therefore did not provide a conductive path to the keeper electrode. A submicron layer of carbon, however, was found on the

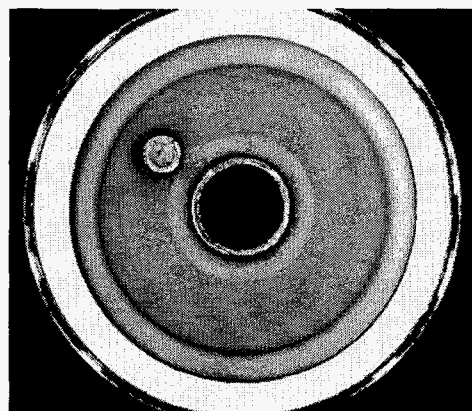


Figure 27. Neutralizer insulator downstream surface showing carbon deposition (brown).

downstream surface of the ceramic, and a conductive path from the central cathode tube to the surrounding keeper tube is visible in Figure 27. Although the coating was too thin to measure its thickness quantitatively with EDX analysis, a resistivity calculation made along the conductive path indicates that a C coating on the order of 25 to 30 Å is sufficient to provide the measured EOT impedance. This finding is critical in that it shows impedance degradation between neutralizer-common and -keeper to be a purely facility-induced effect that would not occur if the engine were operated in the vacuum of space.

As mentioned previously, neutralizer-keeper-to-ground impedance reduced dramatically during the first 2000 hrs of operation and was in the $k\Omega$ range at the conclusion of the test. Inspection of the electrical path from the ground connection to the keeper electrode also indicated the presence of a C coating providing a path from the keeper to the tank-grounded inner cylinder (Figure 28). In addition to the carbon path from keeper to ground, what appears to be melted braze material in the vicinity of the keeper wire termination was found between the concentric keeper and grounded cylinders. An IR thermal scan was performed to see if this area of re-deposited braze material was providing a conductive path from keeper to ground. The thermal scan indicated that the region of the feed-through where the re-deposited braze material was found appeared hotter than the surrounding area. Therefore, the re-deposited braze, in conjunction with the C deposition on the Mo collar, was responsible for the conductive path across the ceramic and the resultant impedance degradation. It is believed that the braze material found surrounding the feed-through was a result of the nominal manufacturing process. If so, this represents a quality-control issue for future NSTAR neutralizer fabrications.

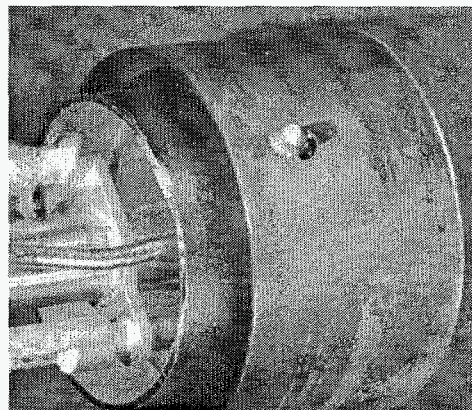


Figure 28. Carbon deposition (blue) on neutralizer ground potential inner cylinder.

VI. Conclusion

In Over 30,352 hours of operation and 235 kg of xenon propellant were processed by the DS1 flight spare ion thruster prior to the voluntary termination of the ELT on June 26, 2003. Significant discharge-cathode-keeper erosion continued through to the end of the test, fully exposing the cathode heater and orifice plate. In spite of this, ignition and discharge characteristics remained unchanged and stable when compared to BOL data. The neutralizer continued to perform well through the end of the final TH5 test segment, with no loss of flow-rate margin from plume mode.

An extensive post-test analysis of the discharge and neutralizer cathode assemblies was performed. Examination of the discharge-cathode assembly revealed that discharge-cathode-keeper erosion had resulted in severe erosion of the cathode-orifice plate, including removal of the plate-to-tube weld. Keeper erosion also resulted in erosion of the cathode-heater outer sheath. Keeper erosion also resulted in flaking of the heater radiation shield, resulting in large Ta flakes adhered to the cathode-tube wall. These findings show that future ion engine designs must eliminate cathode-keeper erosion in order to prevent wear processes that will ultimately result in cathode failure. A semiquantitative analysis of the discharge-cathode insert revealed a clean ID surface with no measurable tungstate or oxide poisoning layers on this surface that would prevent the migration of subsurface impregnate material to the surface. A 60% depletion depth was also measured via a direct comparison to an unused insert, suggesting that the FT2 insert had not yet reached the end of its useful life. Another notable finding was arc damage to the discharge-cathode low-voltage propellant isolator. The arc damage is believed to have been caused by operation outside of its design limitations. Examination of the neutralizer cathode assembly revealed an insert cleaner and less depleted due to its lower current operation. Another notable findings included significant erosion to the keeper tube on the beam exposed side, although the plate to tube weld was intact. Inspection of the neutralizer insulating surfaces confirmed that in-test impedance degradation was a facility induced effect, and would not occur in space.

Acknowledgments

The author would like to acknowledge Norm Hill, Rich Schafer, and Wayne Ohlinger of the Georgia Institute of Technology for performing the SEM and EDX analysis of inserts. The author would also like to acknowledge James Kulleck and Lois Lewis of the Jet Propulsion Laboratory for assisting in the cathode assembly piece-part optical and SEM inspections. Jet Propulsion Laboratory, California Institute of Technology carried out the research described in this paper, under a contract with the National Aeronautics and Space Administration..

References

- ¹ Sengupta, A., Brophy, J. R., Anderson, J. R., Garner, C., de Groh, K., Karniotis, T., and Banks, B., "An Overview of the Results from the 30,000 Hr Life Test of Deep Space 1 Flight Spare Ion Engine," AIAA-2004-C3608C, presented at the 40th AIAA/ASME/SAE/ASEE Joint Propulsion Conference, Ft. Lauderdale, FL, Jul. 2004..
- ² Sengupta, A., et. al., "The 30,000-Hour Extended-Life Test of the Deep Space 1 Flight Spare Ion Thruster, Final Report," NASA/TP 2004-213391, November 2004.
- ³ Sengupta, A., Brophy, J. R., and Goodfellow, K. D., "Status of the Extended Life Test of the Deep Space 1 Flight Spare Ion Engine after 30,352 Hours of Operation," AIAA-2003-4558, presented at the 39th AIAA/ASME/SAE/ASEE Joint Propulsion Conference, Huntsville, AL, Jul. 2003.
- ⁴ Polk, J. E., et al., "The Effect of Engine Wear on Performance in the NSTAR 8000 Hour Ion Engine Endurance Test," AIAA-97-3387, presented at the 33rd AIAA/ASME/SAE/ASEE Joint Propulsion Conference, Seattle, WA, Jul. 1997.
- ⁵ Polk, J. E., Anderson, J. R., Brophy, J. R., Rawlin, V. K., Patterson, M. J., Sovey, J., and Hamley, J., "An Overview of the Results from an 8200 Hour Wear Test of the NSTAR Ion Thruster," AIAA-99-2446, presented at the 35th AIAA/ASME/SAE/ASEE Joint Propulsion Conference, Los Angeles, CA, Jun. 1999.
- ⁶ Polk, J. E., Patterson, M. J., Brophy, J. R., Rawlin, V. K., Sovey, J. S., Myers, R. M., Blandino, J. J., Goodfellow, K. D., and Garner, C. E., "A 1000-Hour Wear Test of Cthe NASA NSTAR Ion Thruster,"C AIAA-96-27C17C, presented at the 32nd AIAA/ASME/SAE/ASEE Joint Propulsion Conference, Lake Buena Vista, FL, Jul. 1996.
- ⁷ Sengupta, A., et al., "Performance Characteristics of the Deep Space 1 Flight Spare Ion Thruster Long Duration Test after 21,300 Hours of Operation," AIAA 2002-3959, Jul. 2002.
- ⁸ Anderson, J. R., et al., "Results of an On-Going Long Duration Ground Test of the DS1 Flight Spare Ion Engine," AIAA-99-2857, presented at the 35th AIAA/ASME/SAE/ASEE Joint Propulsion Conference, Los Angeles, CA, Jun. 1999.
- ⁹ Kolasinski, R. D., and Polk, J. E., "Characterization of Cathode Keeper Wear by Surface Layer Activation," AIAA-2003-5144, Jul. 2003.
- ¹⁰ Brophy, J. R., Brinza, D. E., Polk, J. E., Henry, M. D, and Sengupta, A., "The DS1 Hyper-Extended Mission," AIAA-2002-3673, presented at the 38th AIAA/ASME/SAE/ASEE Joint Propulsion Conference, Indianapolis, IN, Jul. 2002.
- ¹¹ Palluel, P., and Shroff, A. M., "Experimental Study of Impregnated Cathode Behavior, Emission, and Life," *J. Appl. Phys.* 51(5), May 1980.